

Importance of interfacial coupling on the formation and growth of metastable phases

F. Celestini and A. ten Bosch

Laboratoire de Physique de la Matière Condensée, CNRS URA 190, Parc Valrose, 06108 Nice Cedex 02, France

(Received 24 January 1994)

The dynamics of first-order phase transitions are investigated. In many cases, three phases can occur simultaneously, with a finite layer of stable or metastable phases forming at the surface. We present a theory for the formation and growth of metastable phases in planar and spherical geometry. The dynamical equations are based on the time-dependent Landau-Ginzburg equation and can be solved analytically. An exponential interaction term between interfaces is shown to occur and acts to stabilize the metastable surface film. The conditions on the exterior parameters for the appearance of dynamic or static metastable states are given.

PACS number(s): 64.60.My

I. INTRODUCTION

Progress in experimental techniques has led to new results on surface transition phenomena and the papers published on the subject are numerous. For example, observation of the atomic structure of a metallic cluster was possible by scanning tunneling microscopy [1] or, using light scattering, the front velocity during a phase transition was measured in a binary fluid mixture [2]. From a theoretical point of view, the Ginzburg-Landau equation based on an expansion of the free energy in a system specific order parameter is often used to obtain a qualitative understanding of these phenomena. Metiu, Kitahara, and Ross [3] have shown that this model can be derived from the master equation and that front propagation for a steady-state solution is simple to calculate. In this case, the velocity of the propagating front is directly proportional to the undercooling. Often only the static solution for coexisting phases is considered [4], and a mechanical analogy in terms of a fictive Hamiltonian is possible. Among the first to invoke interaction between interfaces, Meister and Muller-Krumbhaar [5] presented a version of "dynamical disordering" leading to a divergence of the width of the propagating interface for a system undergoing a phase transition between two states. Recently, in a numerical study, Bechhoefer, Löwen, and Tuckerman [6] proposed an alternative dynamical mechanism for the production of metastable states. In the present work, we will show how a generalization of this result is possible from the study of the dynamical splitting in a nonequilibrium version of surface melting and wetting.

We consider a system undergoing a first-order phase transition between two states in the presence of an intermediary metastable phase. In a first step, we present an analytical solution of the dynamical problem which is

then extended by introduction of new external parameters. The study of the influence of these parameters on the propagating interface between two phases will lead to the definition of conditions necessary for the appearance of the metastable phase. An interaction term between the two interfaces is shown to occur and an alternative formalism can be defined, which allows simple analytical solutions and a different physical understanding of this type of phenomenon. In the conclusion we will give some applications and extensions of the model.

II. ANALYTICAL SOLUTION

We first study the possibility of formation of an intermediary metastable phase during a phase transition between two states. We solve for the space-time evolution of a nonconserved order parameter $n(z, t)$. The most probable evolution follows the time-dependent Ginzburg-Landau (TDGL) equation. For nucleation on a plane (space coordinate z), and, for simplicity, the mobility and elastic constant set to 1, $n(z, t)$ is a solution of the equation

$$\frac{dn}{dt} = \frac{d^2n}{dz^2} - \frac{df_0}{dn} \quad (1)$$

The potential $f_0(n)$ is a three-well potential representing three states of the system denoted by $n=0, 1$, and 2 . A steady-state solution exists describing the propagation with constant velocity v_{02} of the front separating the states $n=2$ at $z \rightarrow -\infty$ and $n=0$ at $z \rightarrow +\infty$. On transformation of the variable $z \rightarrow z - v_{02}t$ we write (1) as

$$\frac{d^2n}{dz^2} + v_{02} \frac{dn}{dz} - \frac{df_0}{dn} = 0 \quad (2)$$

The following potential is used:

$$\frac{df_0}{dn} = \begin{cases} \frac{df_0^+}{dn^+} = n(n-b_1)[n-(1+\delta)] & \text{for } n(z) < 1, \\ \frac{df_0^-}{dn^-} = [n-(1-\delta)](n-1.4)(n-2) & \text{for } n(z) > 1. \end{cases} \quad (3)$$

Introducing a free parameter $\delta \geq 0$, $f_0(n)$ is split into two double-well potentials for which solutions of Eq. (2) are well known [7]. For a positive δ , the potential is a three-well potential and b_1 is a control parameter which determines the free energy difference between the states $n=0$ and $n=1$ and 2. The other unstable state is taken at $n=1.4$ to assure metastability of the $n=1$ state. If we assume b_1 to be related to the temperature variation, $b_1=b_1(T)$, then $b_1=0.6$ corresponds to the coexistence temperature between the states 0 and 2 and $b_1=0.5$ to the coexistence temperature between the states 0 and 1. In the following we vary b_1 in the range $0.6 > b_1$ where the state 2 is the stable state of the system. We now solve

$$\frac{d^2 n^\mp}{dz^2} + v \frac{dn^\mp}{dz} - \frac{df_0^\mp}{dn^\mp} = 0, \tag{4}$$

with $v=v_{12}$ for $n(z) > 1$ and $v=v_{01}$ for $n(z) < 1$. v_{01} and v_{12} are the front velocities associated with the solutions $n^+(z,t)$ and $n^-(z,t)$ for the following boundary conditions:

$$\lim_{z \rightarrow +\infty} (n^+) = 0, \quad \lim_{-\infty} (n^+) = 1 + \delta, \tag{5a}$$

$$\lim_{z \rightarrow +\infty} (n^-) = 1 - \delta, \quad \lim_{-\infty} (n^-) = 2. \tag{5b}$$

The solutions, plotted in Fig. 1, are well known:

$$n^+(z) = \frac{1 + \delta}{1 + e^{\frac{k(z-z_{01})}{\xi_0}}} \quad \text{for } z > 0 \text{ or } n(z) < 1, \tag{6a}$$

$$n^-(z) = (1 - \delta) + \frac{1 + \delta}{1 + e^{\frac{k(z-z_{12})}{\xi_0}}} \quad \text{for } z < 0 \text{ or } n(z) > 1, \tag{6b}$$

where

$$k = \frac{1 + \delta}{\sqrt{2}} = \frac{1 + \delta}{\xi_0}, \quad v_{01} = 1 + \delta - 2b_1, \quad v_{12} = 0.2 - \delta,$$

ξ_0 being the characteristic length of an independent interface.

The two interfaces are localized at z_{01} and z_{12} , respectively. Continuity at $z=0$ of n^+ , n^- , and their derivatives implies

$$z_{01} = -\frac{\ln(\delta)}{k} = -z_{12}. \tag{7}$$

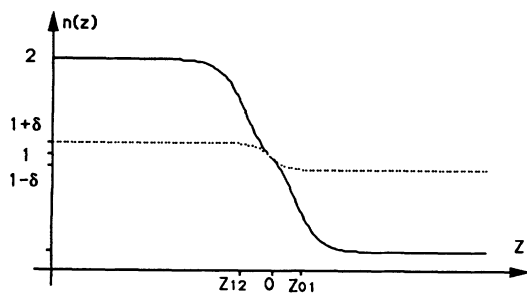


FIG. 1. 20 profile plotted for $\delta=0.15$. The full line represents the front between phases 2 and 0, composed by overlapping of 21 and 10 solutions.

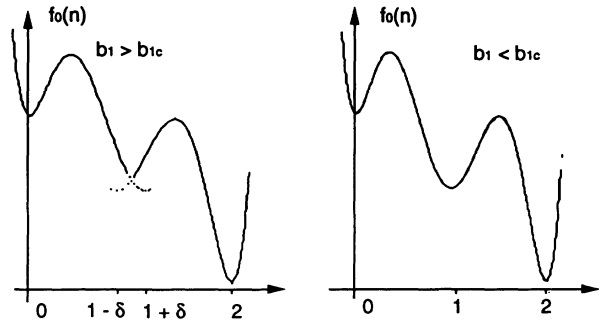


FIG. 2. Potential $f_0(n)$ plotted for two values of the control parameter b_1 . For $b_1 > b_{1c}$ a discontinuity in the derivative of $f_0(n)$ occurs at $n=1$. For $b_1 < b_{1c}$, the potential is a common three-well potential.

The two interfaces must remain at constant relative distance for constant propagation (with velocity v_{02}). The free parameter δ is fixed by the condition $v_{01} = v_{12} = v_{02}$.

$$\delta = \begin{cases} b_1 - 0.4 & \text{for } b_1 > 0.4, \\ 0 & \text{for } b_1 < 0.4. \end{cases} \tag{8}$$

As we can see in Fig. 1, and as confirmed by Eq. (7), the present solution is not possible for $\delta < 0$. For $b_1 < 0.4$, we fix δ to 0 and define a critical value of the model parameter $b_1 = b_{1c} = 0.4$. The potential is plotted for two values of b_1 near b_{1c} in Fig. 2. For $b_1 > b_{1c}$ we obtain an interface between the states 0 and 2 with a constant velocity $v_{02} = 0.6 - b_1$ and an $n=1$ plateau of width $z_{01} - z_{12} = \xi$. For $b_1 \rightarrow b_{1c}$ the width of the $n=1$ front diverges. For $b_1 < b_{1c}$, steady-state propagation of a 02 front is no longer possible. We obtain two independent 01 and 12 profiles with velocities $v_{01} > v_{12}$ so that a macroscopic region of metastable phase is created. The numerical results on dynamical splitting are confirmed (Fig. 3) [6]. The width of the front $\xi = z_{01} - z_{12}$ shows a logarithmic divergence for $b_1 \rightarrow b_{1c}$, as predicted [5] in the case of short range interactions:

$$\xi = z_{01} - z_{12} = \frac{-2 \ln(b_1 - b_{1c})}{k}.$$

The further b_1 lies from the critical value, the smaller the width of the front.

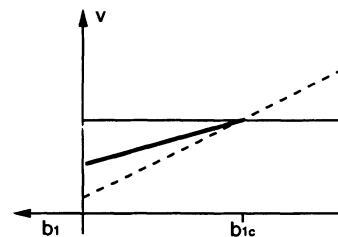


FIG. 3. Velocities of the steady-state solutions: the thick line is for propagation of the 02 front, the dashed line for the 10 front, and the full line, the 21 front. Below the critical point b_{1c} , the 02 front ceases to exist.

III. EFFECT OF MOBILITY AND OF EXTERNAL CONTROL PARAMETERS

We now investigate the effect of the mobility which will enhance dynamical splitting and the production of metastable states. Equation (1) is then (elastic constant again set to 1)

$$\frac{1}{\Gamma(n)} \frac{dn}{dt} = \frac{d^2n}{dz^2} - \frac{df_0}{dn} \tag{9}$$

$$\frac{df_0}{dn} = \begin{cases} \frac{df_0^+}{dn^+} = n^+(n^+ - b_1 n_i)[n^+ - (n_i + \delta)] & \text{for } z > 0, \\ \frac{df_0^-}{dn^-} = [n^+ - (n_i - \delta)][n^+ - n_i - b_2(2 - n_i)](n^+ - 2) & \text{for } z < 0. \end{cases} \tag{10}$$

n_i is the order parameter value for the metastable state, and b_2 is a second control parameter which fixes the energy difference between the states $n = n_i$ and $n = 2$. Depending on the system studied, b_2 can be related to the pressure $b_2 = b_2(P)$ or to the pressure and the temperature $b_2 = b_2(P, T) = b_2(P, b_1)$. At $b_2 = 0.5$ the free energy has the same value for the two states $n = 1$ and 2. We will vary b_2 in the range $0 < b_2 < 0.5$ to conserve metastability of the intermediary state $n = n_i$. The same method described above is used to calculate the O2 front,

$$n^+(z) = \frac{n_i + \delta}{1 + e^{k^+(z - z_{01})}} \tag{11a}$$

$$n^-(z) = (n_i - \delta) + \frac{\delta - n_i + 2}{1 + e^{k^-(z - z_{12})}} \tag{11b}$$

The O2 front exists only for positive values of δ ,

$$\delta = \frac{\Gamma_0(2n_i b_1 - n_i) + \Gamma_2(2 - n_i + 2n_i b_2 - 4b_2)}{\Gamma_0 + \Gamma_2}.$$

We study the influence of the parameters b_2, n_i and the ratio Γ_0/Γ_2 on the existence of the O2 front and on the possibility of producing a dynamic metastable state.

In Fig. 4, we plot the (b_1, b_2) phase diagram and show

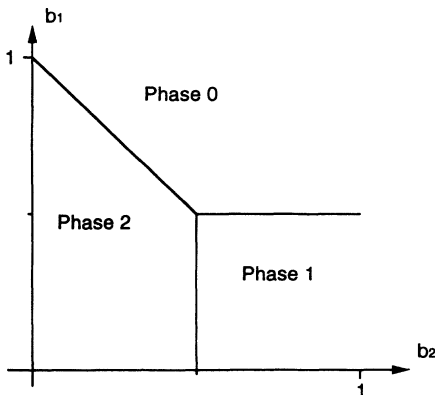


FIG. 4. Phase diagram for the system. We show the different zones of stability for the three states.

$\Gamma(n)$ is the mobility of the system which is assumed to be a function of the order parameter, here taken as a step function,

$$\Gamma(n) = \begin{cases} \Gamma_0 & \text{for } n(z) < n_i, \\ \Gamma_2 & \text{for } n_i < n(z) < 2. \end{cases}$$

We also use a more general form of potential which allows variation of three external model parameters b_1, b_2, n_i :

the three respective zones of stability for the three states. We first examine the influence of the second control parameter b_2 on dynamical splitting. We set $n_i = 1, \Gamma_0 = \Gamma_2 = 1$, and plot in Fig. 5 the boundary for the existence of a O2 front. If the 0 phase is quenched to below this boundary, the O2 front will split and the metastable 1 phase propagates separately and faster than the stable 2 phase. For $b_2 \rightarrow 0.5$ the relative energy between the states 2 and 1 is reduced. The minimum "jump" in control parameter space decreases as b_2 tends to 0.5, as expected when the two states are close in energy.

We explore the influence of the value of the metastable state n_i , setting the mobilities to 1. In Fig. 6 we plot the boundary for existence of an O2 interface for different values of n_i . On increasing the n_i value, the minimum jump in b_1 decreases and the zone of existence of a separate intermediate state is enlarged. If $n_i < 1$ and for values of $b_2 < b_{2c}$ with $b_{2c} = (1 - n_i)/(2 - n_i)$, the O2 front will never split. We see here that if the metastable state is higher in energy than the stable 2 state and the value of the order parameter of the metastable state is far removed from the value of the stable 2 state, dynamical

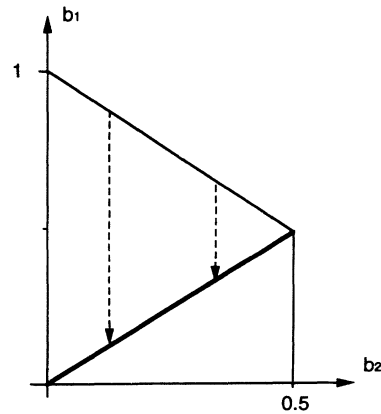


FIG. 5. $\Gamma_0 = \Gamma_1 = 1$ and $n_i = 1$. The thick line represents the boundary for the existence of the O2 front. Two different minimum "jumps" necessary to produce a distinct metastable state are plotted. When the 1 and 2 states are close in energy ($b_2 \rightarrow 0.5$), the amount of quenching is reduced.

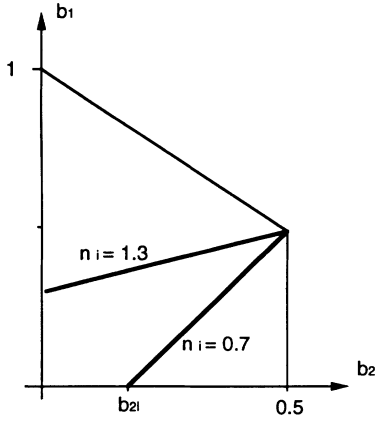


FIG. 6. $\Gamma_0 = \Gamma_1 = 1$. Two boundaries for existence of the O2 interface are plotted for two different values of n_i . An increase in the value of n_i enlarges the zone for appearance of dynamical splitting. For values of $n_i < 1$ and $b_2 < b_{2l}$ we see that dynamical splitting is not possible.

splitting is not possible.

Finally we study the influence of the mobility. For $n_i = 1$ we plot in Fig. 7 the three boundaries for three values of the ratio $R = \Gamma_0/\Gamma_2 > 1$ which correspond to physical situations (for example, the 0 state is a liquid and the 2 state is a solid with crystalline order and a mobility several orders of magnitude smaller than in the liquid). An increase in the value of R decreases the change of external parameters necessary for appearance of the intermediary phase. For high values of R , the boundary tends to the line $b_1 = 0.5$, which corresponds to the transition between the 0 and 1 states. The calculation of the independent velocities shows that v_{01} is proportional to Γ_0 and v_{12} to Γ_2 . When the O2 front splits into two independent fronts with velocities $v_{01} \gg v_{12}$, the creation of a metastable phase is facilitated. Propagation in a non-perfect medium can lead to effective velocities v_{01e} and v_{12e} which are, for example, a function of the defect concentration. We can expect blocking of the 12 front prop-

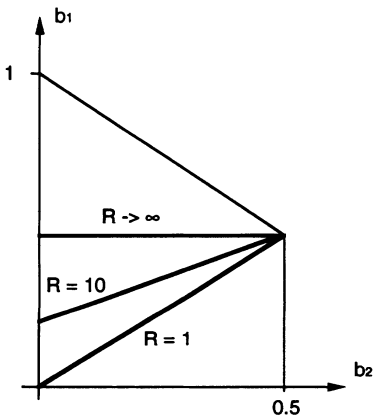


FIG. 7. $n_i = 1$. Three different boundaries are plotted for three different values of the ratio $R = \Gamma_0/\Gamma_2$. An increase of R acts to reduce the minimum quenching.

agating with a low v_{12} value whereas the 10 front continues to propagate.

To summarize, three factors act in favor of the creation of an intermediary metastable state.

(1) The intermediary metastable and the stable states are close in energy.

(2) The relevant order parameters for the intermediary metastable and stable states are close in value.

(3) A high mobility of the initial metastable state compared to the stable state enlarges the zone of external variables for which an intermediary phase 1 occurs and increases the velocity of the 10 front.

It is also possible to consider negative velocities describing dissolution of phase 2 in a phase 0 matrix as well as propagation or dissolution of phase 0 in a phase 2 matrix. The results are similar to those discussed previously. Which of the various dynamic events occurs in a given system will depend on the initial experimental conditions governing the quench.

IV. INTERACTION TERM

In the following we take for simplicity the mobility, the elastic constant, and the position of the intermediary state equal to 1.

We can define a "potential" F_{ij} [which is the Lyapunov function of Eq. (9) [8]] of a front separating the states i and j with profile n_{ij} as

$$F_{ij} = \int_{-\infty}^{+\infty} \left[f_0(n_{ij}) + \left(\frac{dn_{ij}}{dz} \right)^2 \right] dz. \quad (12)$$

For the O2 front, discussed previously, by inserting the solution (6), F_{O2} can be expressed as

$$F_{O2} = F_V(z_{01}, z_{12}) + F_S + I(z_{01}, z_{12}).$$

F_V represents the volume contribution of the free energy and is a function of the positions of the 01 and 12 interfaces. The surface contribution F_S is a constant. $I(z_{01}, z_{12})$ is the interaction term between the two interfaces, already introduced by other means [9] and of vital importance. For example, recent experimental [10] and theoretical [11] work on anisotropic surface melting has been explained on the assumption of an interaction term.

The analytical solutions in (6) lead us to a new derivation for $I(z_{01}, z_{12})$, which is found to be

$$I(z_{01}, z_{12}) = S e^{-k(z_{01} - z_{12})/2} = S e^{-(z_{01} - z_{12})/\xi_i}, \quad (13)$$

where $\xi_i = 2(1 + \delta)/\xi_0$ is the characteristic length of the interaction and S a positive constant. The introduction of the interaction term leads to a new formulation for the TDGL equation in the case of a two-front propagation.

Instead of the exact profile, we can investigate the evolution of the positions z_{ij} and the velocities of the fronts of n_{ij} for $n_{ij} = n_{ij}(z - z_{ij}(t))$ in the limit of $z_{01} - z_{12} > \xi_0$. On integration of Eq. (1) and after some simple manipulations (for details, see Ref. [12]), we find

$$\begin{aligned}
c_{1D} \frac{dz_{01}}{dt} &= - \frac{dF(z_{01}, z_{12})}{dz_{01}}, \\
c_{1D} \frac{dz_{12}}{dt} &= - \frac{dF(z_{01}, z_{12})}{dz_{12}}.
\end{aligned}
\tag{14}$$

F is the static energy described above, which can be written as

$$\begin{aligned}
F(z_{01}, z_{12}) &= F_S + z_{12}(e_2 - e_1) \\
&\quad + z_{01}(e_1 - e_0) + I(z_{01}, z_{12}),
\end{aligned}$$

where $e_i = f_0(n_i)$ is the energy density associated with the uniform phase $i=0, 1, 2$. F_S is the surface energy, independent of z_{01} and z_{12} in one dimension. $F_S = \gamma_{12} + \gamma_{01}$ with γ_{ij} the interfacial energy between states i and j defined as

$$\gamma_{ij} = \int_{-\infty}^{+\infty} \left(\frac{dn_{ij}}{dz} \right)^2 dz.$$

The interaction term $I(z_{01}, z_{12})$ is determined by the spreading coefficient S which can be written in the form

$$S = \gamma_{02} - \gamma_{12} - \gamma_{01},$$

where γ_{02} is the interfacial tension between the states 0 and 2 in the case $\xi=0$ (i.e., $\delta=1$) corresponding to “disappearance” of the intermediary state and a simple double-well potential.

c_{1D} is the effective mobility of the one-dimensional system,

$$c_{1D} = \int_0^{+\infty} \left(\frac{dn^+}{dz} \right)^2 dz = \int_{-\infty}^0 \left(\frac{dn^-}{dz} \right)^2 dz,$$

which after integration gives

$$c_{1D} = \gamma_{01} + \frac{S}{2} e^{k(z_{12} - z_{01})/2} = \gamma_{12} + \frac{S}{2} e^{k(z_{12} - z_{01})/2}.$$

It is now easy to obtain the same analytical results on “dynamical splitting” discussed previously. Furthermore, we can present a different physical interpretation of the phenomenon without the often used mechanical analogy. In this interpretation, the interfaces can be considered as fictitious particles which are subject to different forces. This kind of analogy has been used, for example, in the study of kink-kink or kink-antikink collisions of soliton waves [16]. In our study the interpretation is the following.

The volume free energy leads to a thermodynamic force between the two interfaces. For $b_1 > b_{1c}$, we have an attractive force which is in conflict with the repulsive interaction $I(z_{01}, z_{12})$. An optimal profile can exist and propagates with constant velocity $v_{20} = dz_{12}/dt = dz_{01}/dt$. From Eq. (14), the width of the front is found to be

$$\xi = - \ln \left[\frac{2\xi_i}{S} [2e_1 - e_2 - e_0] \right].$$

When $b_1 \rightarrow b_{1c}$ the attractive force decreases and leads to a large value of the width of the intermediary phase. Fi-

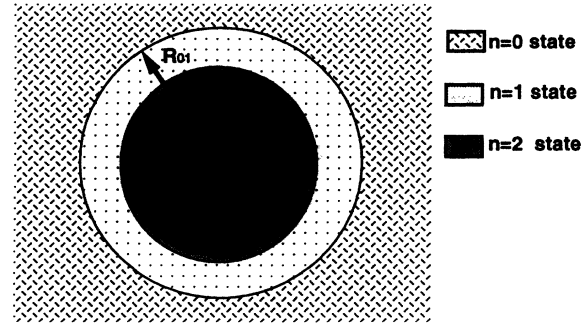


FIG. 8. System in droplet geometry where R_{01} and R_{12} are the positions of the 01 and 12 fronts.

nally, for $b_1 < b_{1c}$, the volume contribution gives a second repulsive term and the two fronts propagate independently. The critical value of the control parameter b_{1c} corresponds to equality of the free energy differences $(e_1 - e_2) = (e_0 - e_1)$. When the free energy difference between the states 0 and 1 is higher than between the states 1 and 2, dynamical splitting occurs. We can also remark that the presence of the interaction term in the effective mobility reduces the speed of relaxation. Note that the criterion for the appearance of the dynamical splitting is given here for a system with equal mobilities, etc. A generalization to a more complex model can easily be performed in the same formalism.

Following the same method [12] combined with work of Chan [13], it is possible to extend to a system of droplet geometry (Fig. 8). The equations are in this case

$$\begin{aligned}
c_{3D} R_{01}^2 \frac{dR_{01}}{dt} &= - \frac{dF_{3D}(R_{01}, R_{12})}{dR_{01}}, \\
c_{3D} R_{12}^2 \frac{dR_{12}}{dt} &= - \frac{dF_{3D}(R_{01}, R_{12})}{dR_{12}}.
\end{aligned}
\tag{15}$$

The potential for the three-dimensional (3D) system is fitted to the expression

$$\begin{aligned}
F_{3D}(R_{01}, R_{12}) &= R_{12}^3 (e_2 - e_1) + R_{01}^3 (e_1 - e_0) \\
&\quad + \gamma_{12} R_{12}^2 + \gamma_{01} R_{01}^2 \\
&\quad + S \left[\frac{R_{01} + R_{12}}{2} \right]^2 e^{-(R_{01} - R_{12})/2\xi_0}
\end{aligned}
\tag{16}$$

and c_{3D} is defined as before [12].

This model is valid in the case of $R_{ij} \gg \xi_0$ and in the absence of thermal effects for a system not subject to heat absorption (or emission). For large droplets, the surface term can be neglected [13] and the results of one-dimensional propagation are valid. The effect of the spherical symmetry is evident in the existence of two critical radii for the two fronts. A static illustration is given in Ref. [11] and an application to a dynamical system is in progress. To illustrate this model, we plot in Fig. 9 the dynamical behavior of an initial droplet characterized by initial positions R_{01} and R_{12} of the 01 and 12 fronts, respectively.

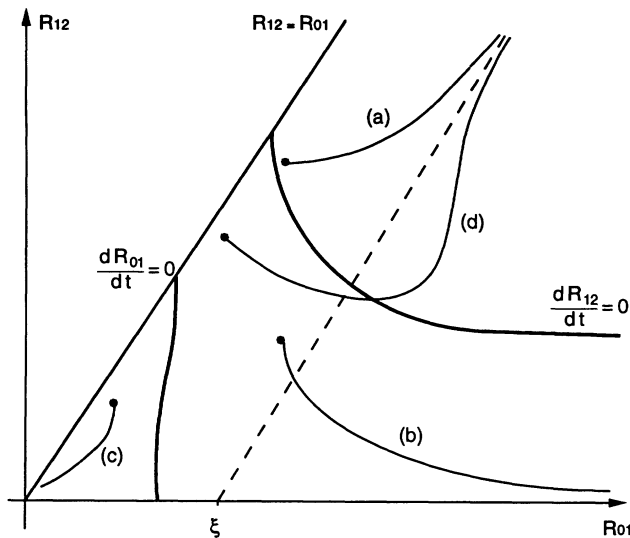


FIG. 9. Numerical solutions of the dynamical equation for a fixed value of the free energy potential (fixed external parameters). The two thick lines represent the two critical radii R_{01c} and R_{12c} . Four paths are plotted in R_{01}, R_{12} space for four different initial conditions. (a) The front tends toward the asymptotic solution given by the one-dimensional case ($R_{01} - R_{12} = \xi$). (b) The 12 front vanishes and the 01 front increases in extension. This illustrates the case where the initial conditions act to create a macroscopic region of the metastable state. (c) The two fronts disappear; no production of the 1 or 2 state is possible. (d) As in the (a) case the fronts tend toward the one-dimensional solution. In this case the position of the 12 front decreases to the value of the critical radius and then increases to the asymptotic solution.

V. CONCLUSION

The analytical solution with the new external parameters introduced in this work can be applied to a specific example of a phase transition for which three phases could exist and then related to experiment. For this purpose, the introduction of a second-order parameter may be necessary [14].

As discussed above, generalization of the problem to systems of higher dimension (droplets) is possible. The

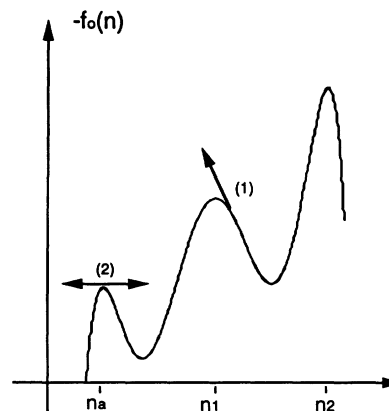


FIG. 10. In the mechanical analogy $-f_0(n)$ is plotted. The fictive particle starts at the bottom of the n_2 well. A third well exists in $n = n_a$ [position (2)]. To fulfill the required boundary condition the particle must arrive at (2) with a zero value of velocity after passing position (1).

introduction of a nonuniform temperature field would be more realistic [15] although the effect on the propagation is generally small in most cases of experimental interest.

The idea of the interaction term between interfaces has already been introduced in the case of surface melting [17] and wetting transitions. The phenomenon described in the present work is just the nonequilibrium version of these phenomena as indicated by Tuckerman and Bechhoefer [14]. To illustrate this point, we can show how the model can be extended to the case of a surface transition between two states in the presence of a substrate or enclosing matrix (as on application of an external field [18]): the order parameter and the derivative are usually fixed at the boundary and the associated profile is calculated from Eq. (1). Referring to the mechanical analogy, we can see (Fig. 10) that fixing the values of n and dn/dz in a point is equivalent to the definition of a new third equilibrium state of the system at $z \rightarrow -\infty$. By definition of a third "absorbed" state, the results of the three-phase model with fixed position of one interface can be applied and the surface transition can then be studied as a function of the energy of the new state.

- [1] J. O. Bovin and J. O. Malm, *Z. Phys. D* **19**, 293 (1991).
- [2] A. Cumming, P. Wiltzius, F. Bates, and J. H. Rosedale, *Phys. Rev. A* **45**, 885 (1992).
- [3] H. Metiu, K. Kitahara, and J. Ross, *J. Chem. Phys.* **64**, 297 (1976).
- [4] B. Widom, in *Liquids, Freezing and the Glass Transition*, edited by J.-P. Hansen, D. Levesque, and J. Zinn-Justin (North-Holland, Amsterdam, 1991), Chap. 6.
- [5] T. Meister and H. Muller-Krumbhaar, *Phys. Rev. Lett.* **51**, 1780 (1983).

- [6] J. Bechhoefer, H. Lowen, and L. S. Tuckerman, *Phys. Rev. Lett.* **67**, 1266 (1991).
- [7] E. W. Montroll, in *Statistical Mechanics*, edited by S. A. Rice *et al.* (University of Chicago, Chicago, 1972).
- [8] N. Minorsky, *Non Linear Oscillations* (Krieger, 1974).
- [9] C. D. Beaglehole, *J. Cryst. Growth* **112**, 663 (1991).
- [10] R. Kofman, P. Cheyssac, R. Garrigos, Y. Lereah, and G. Deutscher, *Z. Phys. D* **20**, 267 (1991).
- [11] A. ten Bosch and F. Celestini, *Z. Phys. D* **28**, 293 (1993).
- [12] M. Mouti and A. ten Bosch, *J. Chem. Phys.* **99**, 1796

- (1993).
- [13] S. K. Chan, *J. Chem. Phys.* **67**, 5755 (1977).
- [14] L. S. Tuckerman and J. Bechhoefer, *Phys. Rev. A* **46**, 3178 (1992).
- [15] S. A. Schofield and D. W. Oxtoby, *J. Chem. Phys.* **94**, 2176 (1991).
- [16] See, for example, O. Legrand, *Phys. Rev. A* **36**, 5068 (1987).
- [17] M. E. Fisher and A. J. Jin, *Phys. Rev. B* **44**, 1430 (1991); D. J. Bukman *et al.*, *ibid.* **47**, 1577 (1993).
- [18] L. Bocquet and H. Lowen, *Phys. Rev. E* **49**, 1883 (1994).

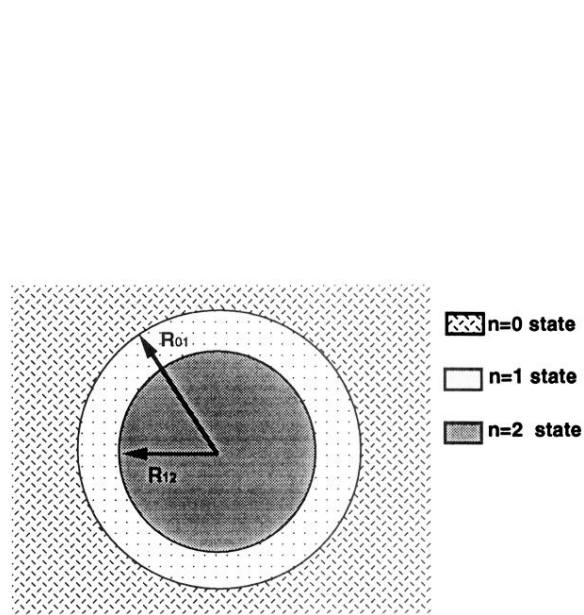


FIG. 8. System in droplet geometry where R_{01} and R_{12} are the positions of the 01 and 12 fronts.